



NIH PUBLIC ACCESS

Author Manuscript

Dev Cell. Author manuscript; available in PMC 2010 December 1.

Published in final edited form as:

Dev Cell. 2010 June 15; 18(6): 950–960. doi:10.1016/j.devcel.2010.02.019.

The Tripartite Motif Protein MADD-2 Functions with the Receptor UNC-40 (DCC) in Netrin-Mediated Axon Attraction and Branching

Joe C. Hao^{1,2,6}, Carolyn E. Adler^{1,4,6}, Leslie Mebane³, Frank B. Gertler³, Cornelia I. Bargmann^{1,4,*}, and Marc Tessier-Lavigne^{2,5,*}¹Howard Hughes Medical Institute, Department of Anatomy and Department of Biochemistry and Biophysics, Program in Neuroscience, University of California, San Francisco, San Francisco, CA 94143, USA²Howard Hughes Medical Institute, Department of Biological Sciences, Stanford University, Stanford, CA 94305, USA³Department of Biology, Massachusetts Institute of Technology, Cambridge, MA 02139, USA⁴Howard Hughes Medical Institute, The Rockefeller University, New York, NY 10065, USA⁵Division of Research, Genentech, Inc., South San Francisco, CA 94080, USA

SUMMARY

Neurons innervate multiple targets by sprouting axon branches from a primary axon shaft. We show here that the ventral guidance factor *unc-6* (*Netrin*), its receptor *unc-40* (*DCC*), and the gene *madd-2* stimulate ventral axon branching in *C. elegans* chemosensory and mechanosensory neurons. *madd-2* also promotes attractive axon guidance to UNC-6 and assists *unc-6*- and *unc-40*-dependent ventral recruitment of the actin regulator MIG-10 in nascent axons. MADD-2 is a tripartite motif protein related to MID-1, the causative gene for the human developmental disorder Opitz syndrome. MADD-2 and UNC-40 proteins preferentially localize to a ventral axon branch that requires their function; genetic results indicate that MADD-2 potentiates UNC-40 activity. Our results identify MADD-2 as an UNC-40 cofactor in axon attraction and branching, paralleling the role of UNC-5 in repulsion, and provide evidence that targeting of a guidance factor to specific axonal branches can confer differential responsiveness to guidance cues.

INTRODUCTION

Axon branches are prominent features of most mature neurons. Axon branching can occur by splitting of the motile growth cone at the leading edge of the axon with subsequent axon bifurcation, growth cone pausing followed by later branch formation at the pause site, or de novo sprouting of interstitial branches far from the growth cone (reviewed in Acebes and Ferrús, 2000). The formation and guidance of axon branches often involves signaling between cells, but the molecular mechanisms that initiate branch formation and targeting are incompletely understood. Once formed, axon branches can be guided independently to distinct locations, implying that individual branches can respond differentially to guidance cues.

^{*}Correspondence: marctl@gene.com (M.T.-L.), cori@rockefeller.edu (C.I.B.).⁶These authors contributed equally to this work

SUPPLEMENTAL INFORMATION Supplemental Information includes one figure and Supplemental Experimental Procedures and can be found with this article online at doi:10.1016/j.devcel.2010.02.019.

The traditional axon guidance molecules, both attractants and repellents, can regulate axonal branching as well. For example, axon branching can be stimulated by the growth cone repellent Slit2 or the axon attractant Netrin-1 (Wang et al., 1999; Kalil et al., 2000; Dent et al., 2004; Ma and Tessier-Lavigne, 2007). The growth cone repellent Sema3A can either stimulate or inhibit branching in vitro, depending on the cell type (Bagnard et al., 1998; Bagri et al., 2003; Dent et al., 2004), and the related repellent Sema3F regulates pruning of branches in vivo (Bagri et al., 2003). Eph/ephrin signaling also regulates axonal branching, both positively and negatively (McLaughlin and O'Leary, 2005; Xu and Henkemeyer, 2009).

Netrins, which include the *C. elegans* UNC-6 protein, elicit many distinct responses in neurons. They can attract and repel axons, promote axon outgrowth, regulate synapse formation, and direct cell migration (Ishii et al., 1992; Serafini et al., 1994, 1996; Kennedy et al., 1994; Colamarino and Tessier-Lavigne, 1995; Colón-Ramos et al., 2007). UNC-6 (Netrin) acts through UNC-40 (DCC) receptors for axon attraction (Chan et al., 1996; Keino-Masu et al., 1996), but mere expression of UNC-40 is not sufficient for an attractive response to UNC-6. Some UNC-40-expressing axons are repelled by UNC-6, through the activity of the UNC-5 coreceptor (Hamelin et al., 1993; Hong et al., 1999), and other UNC-40-expressing axons disregard UNC-6 entirely. A switch between DCC-dependent attraction and repulsion in *Xenopus* neurons can be mediated by changes in cAMP, calcium, or laminin signaling, through mechanisms that are not fully understood (Ming et al., 1997; Hong et al., 2000; Hopker et al., 1999). Signaling downstream of UNC-40 (DCC) receptors is mediated by Rac GTPases, Ena/VASP proteins, MIG-10 (Lamellipodin) proteins, p130CAS, and multiple kinases (Forcet et al., 2002; Gitai et al., 2003; Lebrand et al., 2004; Li et al., 2004; Chang et al., 2006; Quinn et al., 2006; Liu et al., 2007). Most of these effectors participate in both attraction and repulsion, leaving unanswered questions as to how distinct developmental outcomes are specified.

To identify mechanisms regulating axonal branching, we searched for genes that affect stereotyped branching of the axon of the ADL neuron in *C. elegans*. We found that this branching is regulated by UNC-6 acting via UNC-40 and by the newly identified tripartite motif (TRIM) protein MADD-2. Our evidence indicates that MADD-2 functions as a specificity factor with UNC-40 for UNC-6-dependent branch formation and attractive axon guidance in vivo. Strikingly, MADD-2 and UNC-40 are targeted to the axon branches that are dependent on these factors for their guidance, providing direct evidence that subcellular localization of guidance proteins helps sculpt axon morphologies. An independent study has identified *madd-2* as a player in UNC-40 signaling in muscle branches [Alexander et al., 2010 (this issue of *Developmental Cell*)].

RESULTS

Mutations in *madd-2*, *unc-6*, and *unc-40* Disrupt Axon Branching

The ADL neurons are a bilaterally symmetric pair of chemosensory neurons that can be visualized with an *srh-220::gfp* transgene. Each ADL neuron has an anterior dendrite and an axon that enters the nerve ring laterally, where it branches to form dorsal and ventral processes of similar length (Figures 1A and 1B). The ADL dendrite, primary axon, and ventral branches form during embryogenesis and are visible at hatching (data not shown).

Mutants with defects in ADL branch formation were identified by direct examination of ADL axon morphology in *srh-220::gfp* animals. The screen yielded eight similar mutants in which the ventral branches of most ADL axons were stunted or absent, while the dorsal branches were entirely normal (Figures 1C and 1D, Table 1, and data not shown). At a lower frequency, these mutations caused a defect in the initial guidance of the ADL axon, leading it to enter the nerve ring ventrally instead of laterally (Figures 1E and 1F and Table 1). Genetic mapping and complementation tests demonstrated that the mutations fell in three genes: *unc-6* (*Netrin*),

unc-40 (DCC), and a new gene that we have determined to be identical to the muscle branching gene *madd-2* (Alexander et al., 2009). Previously characterized alleles of *unc-6* and *unc-40*, including candidate null alleles, exhibited similar ADL defects (Table 1). ADL defects were already apparent in newly hatched animals, suggesting a role in branch formation rather than branch maintenance (Table 1). These results indicate that *madd-2*, *unc-6*, and *unc-40* have a major role in the formation of the ADL ventral branch and a minor role in the guidance of the primary ADL axon.

unc-40; *madd-2* and *madd-2*; *unc-6* mutants had ADL defects that were not enhanced compared to the stronger single mutant (Table 1). The absence of enhancement, along with their similar phenotypes, suggests that *madd-2* acts with *unc-6* and *unc-40* in a common developmental process.

To determine whether *madd-2*, *unc-6*, and *unc-40* affect axon branch formation in other contexts, we examined the branches of mechanosensory neurons. The primary axon of PLM normally extends a ventrally directed branch near the vulva (Figures 1G and 1H). In *madd-2*, *unc-6*, and *unc-40* mutants, these branches were missing or shorter than normal (Figures 1I and 1J; 60%–70% defective branches in null *madd-2*, *unc-6*, and *unc-40* mutants). The AVM axons normally extend a dorsally directed branch in the nerve ring. AVM branching was defective in *madd-2*, *unc-6*, and *unc-40* mutants, with about half of the animals displaying either a severely shortened branch or no branch (data not shown). These results indicate that *madd-2*, *unc-6*, and *unc-40* affect axon branching in multiple cell types.

***madd-2* Acts with *unc-6* (Netrin) and *unc-40* (DCC) in Ventral Axon Guidance**

unc-6 and *unc-40* have major roles in attractive and repulsive axon guidance. In wild-type animals, the AVM sensory axon is attracted to the ventral nerve cord by UNC-6 (Figures 1K, 1L, and 2A). In *madd-2* mutants, as in *unc-6* and *unc-40* mutants, some AVM axons failed to grow ventrally (Figures 1M, 1N, and 2B). Similar defects were observed in the ventral axon guidance and polarization of the HSN motor neuron (see below). In contrast, repulsive dorsal guidance of the DA and DB motor neurons, which is mediated by *unc-5*, *unc-6*, and *unc-40*, was unaffected in *madd-2* mutants (as assessed with an *unc-129::GFP* reporter; $n = 50$). *unc-5* motor neuron defects are also associated with a characteristic uncoordinated movement phenotype that was not observed in *madd-2* mutants. These results suggest that *madd-2* is not essential for *unc-6*-dependent repulsion.

Further characterization of these and other neurons suggested that *madd-2* defects are selectively associated with *unc-6/unc-40* signaling. For example, Wnt signals regulate the early migration of the HSN neurons and the polarity and anterior-posterior guidance of the PLM mechanosensory neurons (Hilliard and Bargmann, 2006; Prasad and Clark, 2006; Pan et al., 2006). HSN cell migration and PLM polarity were normal in *madd-2* mutants, implying that Wnt signaling was spared. Similarly, the nerve ring was located correctly in *madd-2* mutants, indicating that *sax-3* (*Robo*) functions in nerve ring guidance were preserved (Zallen et al., 1998).

To ask in a more directed way whether *madd-2* acts in the *unc-6/unc-40* guidance pathway, we took advantage of the observation that AVM ventral guidance results from two guidance cues acting in concert: the repellent SLT-1 (*Slit*), which acts through the SAX-3 (*Robo*) receptor to direct axons away from dorsal body wall muscles, and the attractant UNC-6 (*Netrin*), which acts through the UNC-40 (*DCC*) receptor to direct them to the ventral midline (Figure 2A; Hedgecock et al., 1990; Hao et al., 2001). Inactivation of either *Netrin* or *Slit* signaling results in mild AVM guidance defects, but loss of both pathways results in a profound ventral guidance defect. Because of their parallel functions, double mutants with *unc-6* or *slt-1* can be used to assign new guidance genes like *madd-2* to either *Netrin* or *Slit* pathways

(Yu et al., 2002). Double mutant combinations between *madd-2* and either *unc-6* or *unc-40* were no more defective than the stronger single mutant, suggesting that these three genes act in the same pathway for AVM ventral guidance (Figure 2B). In contrast, a *madd-2(ky592);slt-1(eh15)* double mutant was severely defective in ventral axon outgrowth, with all axons extending anteriorly in a lateral position (Figure 2C), like *unc-6(ev400)slt-1(eh15)* double mutant animals. These results indicate that *madd-2* has a major role in the AVM *unc-6/unc-40* guidance pathway, but not in the *slt-1/sax-3* pathway.

UNC-40 affects both axon outgrowth and guidance (Gitai et al., 2003; Stein and Tessier-Lavigne, 2001). The outgrowth function of UNC-40 can be examined in AVM using a gain-of-function form of the UNC-40 receptor, myristoylated UNC-40 (MYR::UNC-40), which lacks the extracellular and transmembrane domains. Expression of MYR::UNC-40 in AVM causes excessive outgrowth phenotypes with additional axons, additional axon branches, and enlarged cell bodies (Gitai et al., 2003). Mutations in the *unc-40* effector genes *unc-34*, *ced-10*, *unc-115*, and *mig-10* are potent suppressors of the excessive outgrowth phenotypes (Gitai et al., 2003; Chang et al., 2006), but mutations in *madd-2* did not suppress these defects or the weaker defects in MYR-UNC-40 transgenes in which the P1 or P2 conserved cytoplasmic motifs were deleted (Figure 2D). These results suggest that the outgrowth-promoting activity of MYR::UNC-40 does not require *madd-2*.

***madd-2* Encodes a Multidomain Protein Similar to Mammalian TRIM Proteins**

Genetic mapping, rescue of the mutant phenotype, and sequencing of mutant alleles identified the predicted transcript C39F7.2 as *madd-2* (Figure 3 and Experimental Procedures; see Supplemental Information available online). A full-length cDNA of *madd-2* is predicted to encode a protein of 751 amino acids. MADD-2 belongs to the large family of TRIM proteins, which encompasses 68 members in humans and 18 in *C. elegans* (Sardiello et al., 2008). MADD-2 has protein-protein interaction motifs including a RING finger, two B-Boxes, and a coiled-coil domain, which together form a so-called RING-B-box-coiled coil (RBCC) or TRIM domain, together with a fibronectin type 3 repeat (FN3) and a C-terminal domain related to domains in the splA kinase and ryanodine receptor (SPRY) (Figure 3C). There are highly conserved homologs of *madd-2* in *Drosophila* (CG31721) and mammals (Figures 3C and 3D). MADD-2 shows strongest similarity along its entire length to two mammalian family members, TRIM9 and TRIM67 (Figures 3C and 3D and data not shown).

The *madd-2* alleles *ky592* and *ky602* contained mutations that create amber stop codons at amino acids 388 and 431, respectively, truncating the predicted protein in the coiled-coil domain (Figure 3C). These two alleles are likely to represent strong loss-of-function mutations in *madd-2*. The *ky580* allele contained a ten nucleotide deletion in the SPRY domain, creating a frameshift in the coding sequence (Figure 3C). ADL branching defects in *ky580* were not as severe as the two putative null alleles, suggesting that *ky580* represents a weaker *madd-2* allele and that an intact SPRY domain is required for full MADD-2 activity (Figure 3C and Table 1; Figure S1).

MADD-2 Is Expressed in the Developing Nervous System

A rescuing *madd-2::gfp* transgene was expressed in most neurons, in hypodermis, and in muscle cells (Figure 4). In many neurons, *madd-2::gfp* expression was transient, peaking during periods of axon outgrowth and guidance. *madd-2::gfp* was most widely and strongly expressed in the embryo, particularly during the initial period of axon outgrowth at 350–400 min of development (Figure 4A, bottom embryo). At this stage, *madd-2::gfp* was prominent in the anterior embryo, including the developing neurons of the nerve ring, in the developing motor neurons of the ventral nerve cord, in posterior neurons, and in hypodermal cells. In most cells, MADD-2::GFP protein was in irregular puncta in the cytoplasm. At ~430 min of

development (1.5-fold stage), the *madd-2::gfp* transgene exhibited a more restricted pattern of expression in the anterior, ventral, and posterior regions of the embryo (Figure 4A, top embryo). The extinction of reporter gene expression in many neurons coincides with the period when most axons in the nerve ring and ventral cord have reached their targets.

At the first larval stage, continued high expression of the *madd-2::gfp* transgene was observed in some head neurons (Figure 4B, arrow), head muscles (Figure 4B, arrowhead), ventral motor neurons, neurons in the tail, and hypodermal cells. As the animals developed from larvae into adults, *madd-2::gfp* expression decreased substantially in head and tail neurons. *madd-2::gfp* expression was detected in the HSN motor neurons around the third larval stage, during the period of its ventral axon outgrowth (Figure 4C, arrow). Although reporter gene fusions should be interpreted with caution, these results suggest that MADD-2 could be present in many Netrin-responsive neurons at the time of axon guidance.

MADD-2 and UNC-40 Preferentially Localize to the Ventral ADL Axon Branch

To determine where *madd-2* functions to direct axon guidance and branching, we expressed a *madd-2* cDNA in specific neurons and tested for rescue of *madd-2(ky592)* defects. MADD-2::GFP expressed under the ADL-specific *srh-220* promoter rescued ADL branching defects in *madd-2(ky592); srh-220::gfp* animals (85% wild-type ADL axons). MADD-2 expressed in the touch cells under the *mec-7* promoter completely rescued the weak AVM ventral guidance defects of *madd-2(ky592)* animals in two out of three transgenic lines (100% wild-type axons, $n \geq 63$ animals/strain). Thus, MADD-2 can function cell autonomously in the ADL neurons in ventral branching and in the AVM neuron in ventral guidance.

In ADL neurons, MADD-2::GFP protein from a rescuing *srh-220::madd-2::gfp* transgene preferentially localized to the ventral branch and not the dorsal branch, both in first-stage larvae and in adults (Figures 4E and 4F; compare *srh-220::GFP* in Figure 4D). The ventral branch consistently contained 4- to 5- fold greater MADD-2::GFP fluorescence intensity than the dorsal branch of the same neuron (Figure 4G, $p < 0.005$ compared to GFP alone). MADD-2::GFP expression was relatively low in the dendrite and primary axon of ADL, but present at high levels in the cell body. The exclusion of MADD-2::GFP from the dorsal ADL branch was preserved in *unc-40* and *unc-6* mutants (0% mislocalized in wild-type, 3% mislocalized in *unc-40(e271)*, and 7% mislocalized in *unc-6(ev400)*; $n = 27-32$). This ventral enrichment is consistent with a localized function of MADD-2 in ventral branching.

A rescuing UNC-40::GFP protein expressed under the *srh-220* promoter was also localized to the ventral branch and not the dorsal branch of ADL in L1 larvae and adult animals (Figure 4H). The dorsal exclusion of UNC-40::GFP was preserved in *madd-2* mutants (5% mislocalized in wild-type, $n = 67$; 4% mislocalized in *madd-2(ky592)*, $n = 49$). Occasional dorsal mislocalization of UNC-40::GFP was observed in *unc-6* mutants (18% mislocalized, $n = 49$). Thus, UNC-40 and MADD-2 are preferentially and independently localized to the ventral branch of ADL.

MADD-2 Potentiates UNC-40 through Its SPRY Domain

madd-2 mutants are systematically less defective in ventral branching and guidance than are *unc-6* and *unc-40* mutants, suggesting that the Netrin pathway retains activity in the absence of *madd-2*. Interestingly, overexpression of UNC-40::GFP protein in ADL neurons rescued the ventral branching defect of *madd-2* mutants nearly completely, such that 90% of ADL neurons had a ventral branch (Table 1; three lines, $n = 73-78$ animals each). In contrast, overexpression of MADD-2 did not suppress an *unc-40* mutation (Table 1). These results suggest that MADD-2 potentiates UNC-40 signaling in axon attraction and branching, but does not signal independently.

The *madd-2(ky580)* allele suggested a potential role for the SPRY domain in MADD-2 function. This protein-protein interaction domain may also link MADD-2 to UNC-40. In vitro-translated MADD-2 associated with a bacterially expressed GST-UNC-40 cytoplasmic domain fusion protein, but not with GST alone or a GST-SAX-3 cytoplasmic domain fusion protein (Figure S1A). The SPRY domain alone was sufficient for this interaction (Figure S1B), which was also confirmed in yeast two-hybrid experiments (Figure S1C). Deletion of the conserved P3 domain of the UNC-40 cytoplasmic domain reduced its binding to MADD-2 in the direct interaction and the yeast two-hybrid assay (Figures S1B and S1C).

The identification of the P3 domain as a potential site of MADD-2 binding matches genetic results. Although genetic experiments in *Drosophila* demonstrate the importance of the conserved P3 domain for axon guidance in vivo (Garbe et al., 2007), the P3 domain is not required for the outgrowth-promoting activity of the MYR::UNC-40 transgene (Gitai et al., 2003). Similarly, *madd-2* was required for guidance in vivo, but not for MYR::UNC-40 activity (Figure 2D).

To ask whether the suggested UNC-40::MADD-2 interaction might be biologically significant, the SPRY domain was deleted from a rescuing *srh-220::madd-2::GFP* clone. Although the expression levels and subcellular distribution of MADD-2(Δ SPRY)::GFP and full-length MADD-2::GFP were similar (Figure S1D), MADD-2(Δ SPRY)::GFP did not rescue ADL branching defects in *madd-2* mutants [30%–41% *madd-2(Aspry)* ADLs had ventral branches, compared with 85% with full-length *madd-2* and 26% in *madd-2* mutant control; three lines, n = 119–135 animals each]. These results support the biological importance of the MADD-2 SPRY domain for UNC-40-dependent branch formation.

MADD-2 Overexpression Causes Ventral Axon Outgrowth and Ectopic Branching in ALM Neurons

The ALM mechanosensory neuron expresses UNC-40 (DCC) (Chan et al., 1996) but is normally neither attracted nor repelled by UNC-6 (Netrin); its lateral axon is unaffected in *unc-40* and *unc-6* mutants (Figures 5A and 5B). A genomic *madd-2::gfp* fusion gene was not detected in ALM neurons of newly hatched larvae (n = 10). When MADD-2 was misexpressed in ALM using the *mec-7* promoter, the ALM axon was redirected toward the ventral UNC-6 cue (Figures 5C and 5D). In rare cases, the ALM axon grew ventrally from its cell body, like the normal AVM axon; more commonly, the ALM axon turned ventrally at a point partway through its trajectory. The ALM cell body was sometimes located in a more ventral position in these animals, suggesting an additional effect of MADD-2 on ALM cell migration (Figures 5E and 5F). MADD-2 overexpression also induced ectopic ventral branching by ALM, demonstrating that it promotes branching in vivo (Figures 5G and 5H).

The effects of MADD-2 overexpression were almost completely suppressed in *unc-40* (*DCC*) mutants, indicating that both the abnormal ventral guidance and the branching caused by MADD-2 require UNC-40 (Figure 5I). Ventral axon outgrowth and cell migration were also suppressed by an *unc-6* mutation, suggesting that *madd-2* expression confers Netrin sensitivity onto ALM (Figure 5I); the excessive branching phenotype was not suppressed. Together, these results suggest that the ALM defects of animals overexpressing MADD-2 arise from inappropriate activation of UNC-40. In agreement with this idea, overexpression of UNC-40 in ALM causes defects similar to those caused by MADD-2 overexpression (Levy-Strumpf and Culotti, 2007).

MADD-2 Acts with UNC-40 to Localize the Effector Protein MIG-10 in HSN

To investigate the acute effects of MADD-2 on UNC-40 signaling, we examined the HSN neuron, whose UNC-6-dependent ventral guidance can be observed in real time (Adler et al.,

2006). The HSN cell body initiates axon formation by polarizing its growth ventrally toward a source of UNC-6 (Figure 6A). A wild-type HSN extends multiple growth cones toward the UNC-6 source during the L3 stage (Figure 6B), whereas those in *unc-6* and *unc-40* mutants extend neurites in all directions. HSN neurons in *madd-2* mutants also extend neurites in all directions (Figure 6C), although the phenotype is weaker than in *unc-6* or *unc-40* mutants (wild-type, 98% ventral growth cones; *madd-2*, 34%; *unc-40*, 11%; *unc-6*, 4%; $n > 100$ animals for each genotype; see also Figure 6I).

One of the first signs of HSN polarization is asymmetric ventral enrichment of the UNC-40 protein in the HSN cell body (Adler et al., 2006). In *madd-2* mutants, UNC-40 accumulated normally at the ventral surface of HSN (Figures 6D and 6E), indicating that in HSN neurons, as in ADL neurons, UNC-40 localization does not require MADD-2.

A later event in UNC-40 signaling in HSN is the ventral localization of MIG-10 (Lamellopodin), a ras-association/pleckstrin homology domain protein that modulates actin dynamics and promotes UNC-40-dependent cytoskeletal remodeling (Krause et al., 2004; Adler et al., 2006; Chang et al., 2006; Quinn et al., 2006). In wild-type animals, MIG-10 segregates strongly to the ventral side of HSN during outgrowth (Figure 6F), but in *madd-2* mutants, MIG-10 was dispersed around the periphery of HSN (Figure 6G). Similar MIG-10 mislocalization is observed in *unc-6* and *unc-40* mutants and in mutants affecting the UNC-40 effectors PI3 kinase, PTEN phosphatase, and Rac (Adler et al., 2006; Quinn et al., 2008; Figure 6H). Thus, MADD-2 is required to localize a signaling component activated by UNC-6 and UNC-40 in HSN.

DISCUSSION

UNC-6 (Netrin) and its receptors UNC-40 (DCC) and UNC-5 have conserved functions in axon guidance, axon outgrowth, cell migration, and cell adhesion. Through a directed screen for branching mutants, followed by a systematic analysis of Netrin-sensitive neurons, we found that the gene *madd-2* affects a subset of *unc-6/unc-40* phenotypes: it affects branching strongly, ventral guidance moderately, and appears not to affect repulsive guidance or outgrowth. Thus MADD-2 appears to have a dedicated role in attractive, and not repulsive, Netrin signaling. We suggest that MADD-2 potentiates UNC-40 or makes it competent for signaling by stabilizing an active UNC-40 conformation, removing an inhibitor, or recruiting effector proteins. The accompanying paper by Alexander et al. (2010) supports a role for MADD-2 in UNC-40-dependent branch formation in a separate cell type, the body wall muscle.

A Role for MADD-2 in Attraction and Branching

Like *unc-6* and *unc-40*, *madd-2* affects the trajectories of several axons that grow ventrally, including AVM and HSN. In AVM, ventral guidance is specified by the cooperative interactions of a ventral attractant, UNC-6, and a dorsal repellent, SLT-1. A *madd-2; slt-1* double mutant loses all AVM ventral guidance, indicating that in the absence of SLT-1 the *madd-2* mutation eliminates any useful attractive information from UNC-6. In most other contexts, however, *madd-2* defects are not as strong as those of *unc-6* and *unc-40*.

Axon guidance has a specific requirement for local receptor activation, with the strongest activation at a site nearest to the highest level of the attractant. The effects of *madd-2* on HSN polarization are consistent with a role in the local activation of UNC-40 signaling. *madd-2* mutant HSNs are poorly polarized by ventral UNC-6 and are defective in the ordered recruitment of MIG-10 to the ventral face of HSN, where high levels of UNC-6 first organize ventral accumulation of UNC-40 protein, and then ventral MIG-10 accumulation that can drive cytoskeletal remodeling (Adler et al., 2006; Krause et al., 2004).

In addition to participating in guidance, MADD-2 also participates in branching. The independent colocalization of MADD-2 and UNC-40 in the same branch of ADL and the gain-of-function phenotypes of MADD-2 in ALM are consistent with a model in which MADD-2 potentiates UNC-40 signaling both in axon attraction and in branching. It is conceivable that these two functions are linked if, for example, the sprouting of a branch is normally triggered by asymmetric presentation of the Netrin cue.

MADD-2 Is a Cofactor for UNC-40 in Attraction, as UNC-5 Is in Repulsion

The roles of MADD-2 in Netrin attraction are reciprocal and complementary to those of UNC-5 in Netrin repulsion. Most notably, MADD-2 and UNC-5 are each sufficient to alter the trajectory of the ALM neuron, which is normally refractory to the ventral UNC-6 cue. Overexpression of UNC-5 in ALM leads to dorsal ALM axon guidance (Hamelin et al., 1993), whereas overexpression of MADD-2 leads to ventral axon guidance and branching. In both cases, endogenous *unc-40* is required for the effects. These results indicate that UNC-5 and MADD-2 can each act as cofactors that define the Netrin responses of an UNC-40-expressing recipient cell: UNC-5 specifies repulsion, whereas MADD-2 specifies attraction and branching.

One significant difference between UNC-5 and MADD-2 is that UNC-5 is a transmembrane receptor that binds Netrin, whereas MADD-2 is a cytoplasmic protein. However, a truncated version of UNC-5 that cannot bind Netrin is still able to convert Netrin attraction to repulsion (Hong et al., 1999). Therefore, the attraction-versus-repulsion outcome can be specified by an intracellular interaction of UNC-5 and UNC-40, which could in principle be similar to the inferred intracellular interaction of UNC-40 and MADD-2.

Functions of TRIM Family Proteins in Development

MADD-2 is a member of the RBCC or TRIM family, defined by an N-terminal RING finger domain, one or two B-box motifs, and a coiled-coil region (reviewed in Sardiello et al., 2008). The RING finger is a cysteine/histidine-rich zinc-binding domain; B-box motifs are zinc-binding domains that are only found within this protein family; and the coiled-coil domain can mediate homomultimerization and localization of TRIM proteins. Several TRIM proteins act as E3 ubiquitin ligases, and a subset of TRIM proteins with RNA-binding domains (not present in MADD-2) interact with miRNA pathways (Slack et al., 2000, Neumuller et al., 2008). Specific TRIM proteins have roles in human developmental disorders, Mendelian disease syndromes, and innate immunity and susceptibility to HIV infection (Quaderi et al., 1997; Stremlau et al., 2004; Sardiello et al., 2008).

MADD-2 also has a fibronectin type III domain and a SPRY domain, a domain structure shared with several vertebrate TRIM proteins including TRIM9, TRIM67, and TRIM18 (MID1). Most fibronectin type III domains are extracellular, but some are present in cytoplasmic proteins such as the axon guidance factor UNC-73 (TRIO) (Steven et al., 1998); the absence of signal sequences or transmembrane domains suggests a cytoplasmic location for MADD-2 and related proteins. *Trim9* mRNA is highly expressed in specific regions in the developing central nervous system (Berti et al., 2002). Consistent with a possible role in axonal development, *Trim9* is expressed highly throughout the mantle layer of the mouse spinal cord, including commissural neurons, at embryonic day 11 when DCC-expressing commissural axons are projecting to the midline and is also expressed in developing dorsal root and trigeminal sensory ganglia (J.C.H., F. Wang, C.I.B., and M.T.L., unpublished data). MADD-2 also shows substantial similarity to the TRIM18 (MID1) protein mutated in the human congenital disorder Opitz G/BBB syndrome, which involves dysgenesis of ventral midline structures and mental retardation associated with dysplasia of the corpus callosum (Quaderi et al., 1997). The biochemical functions of TRIM9, TRIM18, and TRIM67, like those of most TRIM proteins, are

incompletely understood. TRIM9 is enriched at presynaptic nerve terminals of mature neurons (Li et al., 2001). TRIM18 interacts with microtubules and can decrease their depolymerization, an interaction reduced by the mutations that occur in Opitz G/BBB syndrome (Schweiger et al., 1999); it also exhibits a ubiquitin ligase activity that targets protein phosphatase 2A for degradation (Troddenbacher et al., 2001). Our results indicate that the TRIM protein MADD-2 has a specific role in UNC-40 signaling. Whether TRIM9, TRIM18, or TRIM67 functions in DCC signaling in vertebrates remains to be determined.

MADD-2, UNC-40, and the Regulation of Branch Responsiveness

The strong branching defects in *madd-2*, *unc-6*, and *unc-40* mutants indicate that some neurons use *unc-6* signaling to control branching even when their axon guidance is mostly (ADL) or entirely (PLM) independent of UNC-6 activity. *unc-6* had not previously been recognized as a major factor in axon branching, although *unc-6* mutants have been noted to have branching defects when their guidance was disrupted (Hedgecock et al., 1990). However, Netrin-1 can stimulate branch formation of vertebrate cortical axons in vitro (Dent et al., 2004; Tang and Kalil, 2005) and a C-terminally deleted UNC-6 protein causes aberrant motor neuron branching through an UNC-5 and activity-dependent pathway (Lim et al., 1999; Wang and Wadsworth, 2002). The branch-promoting role of *unc-6* may represent one of several mechanisms by which Netrin regulates synapse formation as well as axon guidance (Colón-Ramos et al., 2007).

The fact that individual branches of an axon must be selectively guided, and hence selectively dependent on particular guidance cues, has long been inferred but not directly demonstrated. Our results provide evidence for such selective responses. They also identify a mechanism that can help explain this selectivity, namely, the specific targeting of MADD-2 and UNC-40 to the ventral and not the dorsal branch of ADL. The restricted subcellular localization of guidance receptors provides a powerful mechanism for sculpting guidance patterns (Brittis et al., 2002). Neither MADD-2 nor UNC-40 is required for the localization of the other protein, suggesting that both respond to a common signal that defines the dorsal and ventral axon branches as distinct compartments for protein delivery, local translation, or retention. These results thus provide evidence that targeting of specific effectors to particular branches can confer differential branch responsiveness to guidance cues and provide an entry point for identifying the factors that identify different branches as distinct functional compartments.

EXPERIMENTAL PROCEDURES

Strains and Molecular Biology

Wild-type animals were *C. elegans* variety Bristol, strain N2. Worms were grown at 20°C and maintained using standard methods (Brenner, 1974). Strains used in these studies included: LGI, *unc-40* (*e271*, *e1430*, *ky568*, *ky591*), *kyIs170* [*srh-220::gfp*, *lin-15(+)*], *zdIs5* [*mec-4::gfp*, *lin-15(+)*]; LGIV, *ced-10*(*n1993*), *unc-5*(*e53*), *zdIs4* [*mec-4::gfp*, *lin-15(+)*], *kyIs262* (*unc-86::myr-gfp*, *odr-1::dsRed*); LGV, *madd-2* (*ky580*, *ky592*, *ky602*), *unc-34*(*gm104*), *unc-34*(*e566*), *unc-60*(*e677*), *dpy-11*(*e224*); and LGX, *unc-6* (*ev400*, *ky567*, *ky577*, *ky585*), *sax-3*(*ky123*), *slt-1*(*eh15*), *unc-115*(*ky275*). Transgenes maintained as extrachromosomal arrays included: *kyEx690* [*madd-2*(genomic)::*gfp*, *odr-1::dsRed*], *kyEx688* (*srh-220::madd-2::gfp*, *unc-122::gfp*), *kyEx638* (*mec-7::madd-2*, *odr-1::dsRed*), *kyEx3574* [*srh-220::madd-2::gfp*(*ΔSPRY*), *unc-122::gfp*], *kyEx456* (*mec-7::myr::unc-40*, *str-1::gfp*), *kyEx637* [*mec-7::myr::unc-40*(*ΔP2*), *odr-1::dsRed*], *kyEx639* [*mec-7::myr::unc-40*(*ΔP1*), *odr-1::dsRed*], *kyEx1213* (*unc-86::unc-40::gfp*, *odr-1::dsRed*), *kyEx927* (*unc-86::mig-10::gfp*, *odr-1::dsRed*), *kyEx2077* [*srh-220::unc-40::gfp*, *lin-15(+)*, *unc-122::gfp*]. The *zdIs4* and *zdIs5* strains were kindly provided by S. Clark. Some strains were provided by the Caenorhabditis Genetics Center. Standard methods were used to make plasmids and transgenic strains; detailed information appears in the Supplemental Information.

Characterization of Neuronal Morphology

ADL axonal morphology was visualized using an integrated *srh-220::gfp* transcriptional fusion, *kyIs170* (see Supplemental Information). Touch cell neurons were visualized with the integrated *mec-4::gfp* transgenes *zdlIs4* and *zdlIs5*.

Animals were mounted on 2% agarose pads in M9 buffer containing 5 mM sodium azide and examined by fluorescence microscopy. Images were captured using either a Bio-Rad MRC-1024 confocal microscope, a SPOT camera (RT Slider Diagnostic Instruments, Inc.), or an LSM5LIVE. For some figures, a stack of images was obtained using confocal microscopy and projected into a single plane for presentation.

For HSN experiments, synchronized populations were obtained by allowing eggs to hatch overnight in M9 buffer without food; the resulting L1 nematodes were fed and grown at 25°C to specified developmental stages (Adler et al., 2006).

***madd-2* Mapping**

madd-2 mutant alleles were isolated by direct observation of the ADL axon following EMS mutagenesis (Brenner, 1974) and mapped using transposable element and SNP polymorphisms and genetic deficiencies. Details of mapping, cDNA isolation, and transgenic rescue are in the Supplemental Information.

Quantitation of MADD-2 and UNC-40 Enrichment in Axon Branches

Fluorescence intensity of MADD-2::GFP or UNC-40::GFP was measured on the ADL dorsal and ventral branches using NIH Image software. An area adjacent to either branch was used to determine background fluorescence and subtracted from the fluorescence intensity value for the respective branch. After subtraction of background levels, dividing the fluorescence intensity of the ventral branch by the fluorescence intensity of the dorsal branch generated a ratio for protein enrichment in the ADL ventral branch. For comparison purposes, an identical ratio was determined for ADL neurons expressing GFP alone. In each case, multiple neurons were examined and the mean and standard error of the mean were calculated. t test analyses were performed between ratios determined for GFP only and either MADD-2::GFP or UNC-40::GFP to assess the significance of the enrichment in the ventral branch.

Supplementary Material

Refer to Web version on PubMed Central for supplementary material.

Acknowledgments

We thank G. Hloppeter for assistance with injections and D. Robinson and D. Colon-Ramos for discussions and insights. This work was supported by the Howard Hughes Medical Institute and by National Institutes of Health grant GM0680678. J.C.H. was a Howard Hughes Predoctoral Fellow. C.I.B. and M.T.L. were Investigators of the Howard Hughes Medical Institute.

REFERENCES

- Acebes A, Ferrús A. Cellular and molecular features of axon collaterals and dendrites. *Trends Neurosci* 2000;23:557–565. [PubMed: 11074265]
- Adler CE, Fetter RD, Bargmann CI. UNC-6/Netrin induces neuronal asymmetry and defines the site of axon formation. *Nat. Neurosci* 2006;9:511–518. [PubMed: 16520734]
- Alexander M, Chan KK, Byrne AB, Selman G, Lee T, Ono J, Wong E, Puckrin R, Dixon SJ, Roy PJ. An UNC-40 pathway directs postsynaptic membrane extension in *Caenorhabditis elegans*. *Development* 2009;136:911–922. [PubMed: 19211675]

- Bagnard D, Lohrum M, Uziel D, Puschel AW, Bolz J. Semaphorins act as attractive and repulsive guidance signals during the development of cortical projections. *Development* 1998;125:5043–5053. [PubMed: 9811588]
- Bagri A, Cheng HJ, Yaron A, Pleasure SJ, Tessier-Lavigne M. Stereotyped pruning of long hippocampal axon branches triggered by retraction inducers of the semaphorin family. *Cell* 2003;113:285–299. [PubMed: 12732138]
- Berti C, Messali S, Ballabio A, Reymond A, Meroni G. TRIM9 is specifically expressed in the embryonic and adult nervous system. *Mech. Dev* 2002;113:159–162. [PubMed: 11960705]
- Brenner S. The genetics of *Caenorhabditis elegans*. *Genetics* 1974;77:71–94. [PubMed: 4366476]
- Brittis PA, Lu Q, Flanagan JG. Axonal protein synthesis provides a mechanism for localized regulation at an intermediate target. *Cell* 2002;110:223–235. [PubMed: 12150930]
- Chan SS-Y, Zheng H, Su M-W, Wilk R, Killeen MR, Hedgecock EM, Culotti JG. UNC-40, a *C. elegans* homolog of DCC (Deleted in Colorectal Cancer), is required in motile cells responding to UNC-6 netrin cues. *Cell* 1996;87:187–195. [PubMed: 8861903]
- Chang C, Adler CE, Krause M, Clark SG, Gertler FB, Tessier-Lavigne M, Bargmann CI. MIG-10/lamellipodin and AGE-1/PI3K promote axon guidance and outgrowth in response to slit and netrin. *Curr. Biol* 2006;16:854–862. [PubMed: 16618541]
- Colamarino SA, Tessier-Lavigne M. The axonal chemoattractant netrin-1 is also a chemorepellent for trochlear motor axons. *Cell* 1995;81:621–629. [PubMed: 7758116]
- Colón-Ramos DA, Margeta MA, Shen K. Glia promote local synaptogenesis through UNC-6 (netrin) signaling in *C. elegans*. *Science* 2007;318:103–106. [PubMed: 17916735]
- Dent EW, Barnes AM, Tang F, Kalil K. Netrin-1 and semaphorin 3A promote or inhibit cortical axon branching, respectively, by reorganization of the cytoskeleton. *J. Neurosci* 2004;24:3002–3012. [PubMed: 15044539]
- Forcet C, Stein E, Pays L, Corset V, Llambi F, Tessier-Lavigne M, Mehlen P. Netrin-1-mediated axon outgrowth requires deleted in colorectal cancer-dependent MAPK activation. *Nature* 2002;417:443–447. [PubMed: 11986622]
- Garbe DS, O'Donnell M, Bashaw GJ. Cytoplasmic domain requirements for Frazzled-mediated attractive axon turning at the *Drosophila* midline. *Development* 2007;134:4325–4334. [PubMed: 18003737]
- Gitai Z, Yu TW, Lundquist EA, Tessier-Lavigne M, Bargmann CI. The Netrin receptor UNC-40/DCC stimulates axon attraction and outgrowth through Enabled and, in parallel, Rac and UNC-115/abLIM. *Neuron* 2003;37:53–65. [PubMed: 12526772]
- Hamelin M, Zhou Y, Su MW, Scott IM, Culotti JG. Expression of the UNC-5 guidance receptor in the touch neurons of *C. elegans* steers their axons dorsally. *Nature* 1993;364:327–330. [PubMed: 8332188]
- Hao JC, Yu TW, Fujisawa K, Culotti JG, Gengyo-Ando K, Mitani S, Moulder G, Barstead R, Tessier-Lavigne M, Bargmann CI. *C. elegans* Slit acts in midline, dorsal-ventral, and anterior-posterior guidance via the SAX-3/Robo receptor. *Neuron* 2001;32:25–38. [PubMed: 11604136]
- Hedgecock EM, Culotti JG, Hall DH. The *unc-5*, *unc-6*, and *unc-40* genes guide circumferential migrations of pioneer axons and mesodermal cells on the epidermis in *C. elegans*. *Neuron* 1990;4:61–85. [PubMed: 2310575]
- Hilliard MA, Bargmann CI. Wnt signals and frizzled activity orient anterior-posterior axon outgrowth in *C. elegans*. *Dev. Cell* 2006;10:379–390. [PubMed: 16516840]
- Hong K, Hinck L, Nishiyama M, Poo MM, Tessier-Lavigne M, Stein E. A ligand-gated association between cytoplasmic domains of UNC5 and DCC family receptors converts Netrin-induced growth cone attraction to repulsion. *Cell* 1999;97:927–941. [PubMed: 10399920]
- Hong K, Nishiyama M, Henley J, Tessier-Lavigne M, Poo M. Calcium signalling in the guidance of nerve growth by Netrin-1. *Nature* 2000;403:93–98. [PubMed: 10638760]
- Hopker VH, Shewan D, Tessier-Lavigne M, Poo M, Holt C. Growth-cone attraction to Netrin-1 is converted to repulsion by Laminin-1. *Nature* 1999;401:69–73. [PubMed: 10485706]
- Ishii N, Wadsworth WG, Stern BD, Culotti JG, Hedgecock EM. UNC-6, a laminin-related protein, guides cell and pioneer axon migrations in *C. elegans*. *Neuron* 1992;9:873–881. [PubMed: 1329863]
- Kalil K, Szebenyi G, Dent EW. Common mechanisms underlying growth cone guidance and axon branching. *J. Neurobiol* 2000;44:145–158. [PubMed: 10934318]

- Keino-Masu K, Masu M, Hinck L, Leonardo ED, Chan SS, Culotti JG, Tessier-Lavigne M. Deleted in Colorectal Cancer (DCC) encodes a Netrin receptor. *Cell* 1996;87:175–185. [PubMed: 8861902]
- Kennedy TE, Serafini T, de la Torre JR, Tessier-Lavigne M. Netrins are diffusible chemotropic factors for commissural axons in the embryonic spinal cord. *Cell* 1994;78:425–435. [PubMed: 8062385]
- Krause M, Leslie JD, Stewart M, Lafuente EM, Valderrama F, Jagannathan R, Strasser GA, Rubinson DA, Liu H, Way M, et al. Lamellipodin, an Ena/VASP ligand, is implicated in the regulation of lamellipodial dynamics. *Dev. Cell* 2004;7:571–583. [PubMed: 15469845]
- Lebrand C, Dent EW, Strasser GA, Lanier LM, Krause M, Svitkina TM, Borisy GG, Gertler FB. Critical role of Ena/VASP proteins for filopodia formation in neurons and in function downstream of Netrin-1. *Neuron* 2004;42:37–49. [PubMed: 15066263]
- Levy-Strumpf N, Culotti JG. VAB-8, UNC-73 and MIG-2 regulate axon polarity and cell migration functions of UNC-40 in *C. elegans*. *Nat. Neurosci* 2007;10:161–168. [PubMed: 17237777]
- Li Y, Chin LS, Weigel C, Li L. Spring, a novel RING finger protein that regulates synaptic vesicle exocytosis. *J. Biol. Chem* 2001;276:40824–40833. [PubMed: 11524423]
- Li W, Lee J, Vikis HG, Lee SH, Liu G, Aurandt J, Shen TL, Fearon ER, Guan JL, Han M, et al. Activation of FAK and Src are receptor-proximal events required for netrin signaling. *Nat. Neurosci* 2004;7:1213–1221. [PubMed: 15494734]
- Lim YS, Mallapur S, Kao G, Ren XC, Wadsworth WG. Netrin UNC-6 and the regulation of branching and extension of motoneuron axons from the ventral nerve cord of *Caenorhabditis elegans*. *J. Neurosci* 1999;19:7048–7056. [PubMed: 10436059]
- Liu G, Li W, Gao X, Li X, Jurgensen C, Park HT, Shin NY, Yu J, He ML, Hanks SK, et al. P130CAS is required for netrin signaling and commissural axon guidance. *J. Neurosci* 2007;27:957–968. [PubMed: 17251438]
- Ma L, Tessier-Lavigne M. Dual branch-promoting and branch-repelling actions of Slit/Robo signaling on peripheral and central branches of developing sensory axons. *J. Neurosci* 2007;27:6843–6851. [PubMed: 17581972]
- McLaughlin T, O’Leary DD. Molecular gradients and development of retinotopic maps. *Annu. Rev. Neurosci* 2005;28:327–355. [PubMed: 16022599]
- Ming GL, Song HJ, Berninger B, Holt CE, Tessier-Lavigne M, Poo MM. cAMP-dependent growth cone guidance by Netrin-1. *Neuron* 1997;19:1225–1235. [PubMed: 9427246]
- Neumuller RA, Betschinger J, Fischer A, Bushati N, Poernbacher I, Mechtler K, Cohen SM, Knoblich JA. Mei-P26 regulates micro-RNAs and cell growth in the *Drosophila* ovarian stem cell lineage. *Nature* 2008;454:241–245. [PubMed: 18528333]
- Pan CL, Howell JE, Clark SG, Hilliard M, Cordes S, Bargmann CI, Garriga G. Multiple Wnts and frizzled receptors regulate anteriorly directed cell and growth cone migrations in *Caenorhabditis elegans*. *Dev. Cell* 2006;10:367–377. [PubMed: 16516839]
- Prasad BC, Clark SG. Wnt signaling establishes anteroposterior neuronal polarity and requires retromer in *C. elegans*. *Development* 2006;133:1757–1766. [PubMed: 16571624]
- Quaderi NA, Schweiger S, Gaudenz K, Franco B, Rugarli EI, Berger W, Feldman GJ, Volta M, Andolfi G, Gilgenkrantz S, et al. Opitz G/BBB syndrome, a defect of midline development, is due to mutations in a new RING finger gene on Xp22. *Nat. Genet* 1997;17:285–291. [PubMed: 9354791]
- Quinn CC, Pfeil DS, Chen E, Stovall EL, Harden MV, Gavin MK, Forrester WC, Ryder EF, Soto MC, Wadsworth WG. UNC-6/netrin and SLT-1/slit guidance cues orient axon outgrowth mediated by MIG-10/RIAM/lamellipodin. *Curr. Biol* 2006;16:845–853. [PubMed: 16563765]
- Quinn CC, Pfeil DS, Wadsworth WG. CED-10/Rac1 mediates axon guidance by regulating the asymmetric distribution of MIG-10/lamellipodin. *Curr. Biol* 2008;18:808–813. [PubMed: 18499456]
- Sardiello M, Cairo S, Fontanella B, Balladio A, Meroni G. Genomic analysis of the TRIM family reveals two groups of genes with distinct evolutionary properties. *BMC Evol. Biol* 2008;8:225. [PubMed: 18673550]
- Schweiger S, Foerster J, Lehmann T, Suckow V, Muller YA, Walter G, Davies T, Porter H, van Bokhoven H, Lunt PW, et al. The Opitz syndrome gene product, MID1, associates with microtubules. *Proc. Natl. Acad. Sci. USA* 1999;96:2794–2799. [PubMed: 10077590]

- Serafini T, Kennedy TE, Galko MJ, Mirzayan C, Jessell TM, Tessier-Lavigne M. The Netrins define a family of axon outgrowth-promoting proteins homologous to *C. elegans* UNC-6. *Cell* 1994;78:409–424. [PubMed: 8062384]
- Serafini T, Colamarino SA, Leonardo ED, Wang H, Beddington R, Skarnes WC, Tessier-Lavigne M. Netrin-1 is required for commissural axon guidance in the developing vertebrate nervous system. *Cell* 1996;87:1001–1014. [PubMed: 8978605]
- Slack FJ, Basson M, Liu Z, Ambros V, Horvitz HR, Ruvkun G. The *lin-41* RBCC gene acts in the *C. elegans* heterochronic pathway between the *let-7* regulatory RNA and the LIN-29 transcription factor. *Mol. Cell* 2000;5:659–669. [PubMed: 10882102]
- Stein E, Tessier-Lavigne M. Hierarchical organization of guidance receptors: silencing of Netrin attraction by Slit through a Robo/DCC receptor complex. *Science* 2001;291:1928–1938. [PubMed: 11239147]
- Steven R, Kubiseski TJ, Zheng H, Kulkarni S, Mancillas J, Ruiz Morales A, Hogue CW, Pawson T, Culotti J. UNC-73 activates the Rac GTPase and is required for cell and growth cone migrations in *C. elegans*. *Cell* 1998;92:785–795. [PubMed: 9529254]
- Stremlau M, Owens CM, Perron MJ, Kiessling M, Autissier P, Sodroski J. The cytoplasmic body component TRIM5alpha restricts HIV-1 infection in Old World monkeys. *Nature* 2004;427:848–853. [PubMed: 14985764]
- Tang F, Kalil K. Netrin-1 induces axon branching in developing cortical neurons by frequency-dependent calcium signaling pathways. *J. Neurosci* 2005;25:6702–6715. [PubMed: 16014732]
- Trockenbacher A, Suckow V, Foerster J, Winter J, Krauss S, Ropers HH, Schneider R, Schweiger S. MID1, mutated in Opitz syndrome, encodes an ubiquitin ligase that targets phosphatase 2A for degradation. *Nat. Genet* 2001;29:287–294. [PubMed: 11685209]
- Wang Q, Wadsworth WG. The C domain of netrin UNC-6 silences calcium/calmodulin-dependent protein kinase- and diacylglycerol-dependent axon branching in *Caenorhabditis elegans*. *J. Neurosci* 2002;22:2274–2278. [PubMed: 11896167]
- Wang KH, Brose K, Arnott D, Kidd T, Goodman CS, Henzel W, Tessier-Lavigne M. Biochemical purification of a mammalian Slit protein as a positive regulator of sensory axon elongation and branching. *Cell* 1999;96:771–784. [PubMed: 10102266]
- Xu NJ, Henkemeyer M. Ephrin-B3 reverse signaling through Grb4 and cytoskeletal regulators mediates axon pruning. *Nat. Neurosci* 2009;12:268–276. [PubMed: 19182796]
- Yu TW, Hao JC, Lim W, Tessier-Lavigne M, Bargmann CI. Shared receptors in axon guidance: SAX-3/Robo signals via UNC-34/Enabled and a Netrin-independent UNC-40/DCC function. *Nat. Neurosci* 2002;5:1147–1154. [PubMed: 12379860]
- Zallen JA, Yi BA, Bargmann CI. The conserved immunoglobulin superfamily member SAX-3/Robo directs multiple aspects of axon guidance in *C. elegans*. *Cell* 1998;92:217–227. [PubMed: 9458046]

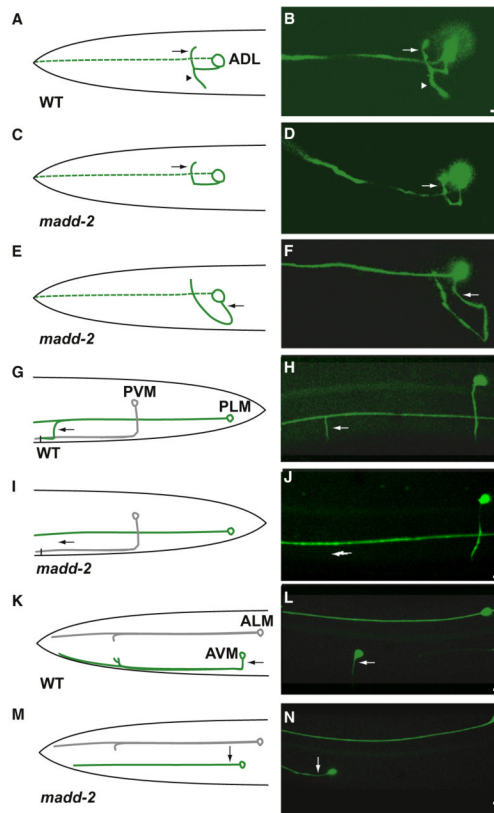


Figure 1. Axon Branching and Guidance Are Disrupted in *madd-2* Mutants

(A–F) ADL neurons visualized with *srh-220::gfp* transgene and schematics.

(A and B) The wild-type ADL cell body projects an axon laterally into the nerve ring, where it branches into a dorsal (arrow) and a ventral (arrowhead) process.

(C and D) *madd-2(ky592)* ADL; normal dorsal branch (arrow) and no ventral branch.

(E and F) *madd-2(ky592)* ADL; defective guidance of the ADL primary axon (arrow) into the nerve ring.

(G–J) PLM neurons visualized with *mec-4::gfp* transgene and schematics. (G and H) The wild-type PLM neuron extends a primary axon anteriorly and projects a ventrally directed axon branch (arrow) near the vulva. (I and J) *madd-2(ky592)* PLM defective in ventral branch (arrow).

(K–N) AVM neurons visualized with *mec-4::gfp* transgene and schematics. (K and L) The wild-type AVM axon projects ventrally (arrow) and then extends anteriorly. (M and N) *madd-2(ky592)* AVM axon growing anteriorly (arrow) in a lateral position instead of ventrally.

Anterior is to the left and dorsal is at the top in all panels. Scale bars, 2 μ m.

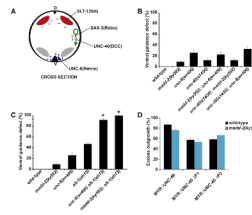


Figure 2. *madd-2* Acts in the *unc-6/unc-40* Pathway for AVM Ventral Guidance

(A) AVM ventral guidance. The expression of both SAX-3 (Robo) and UNC-40 (DCC) receptors in AVM (green) allows its axon to extend toward the ventral UNC-6 (Netrin) attractive cue (blue) made by neurons and away from the dorsal SLT-1 repulsive cue made by muscles (red). Ventral muscles are shown in gray.

(B and C) AVM ventral guidance defects in single and double mutants, scored using a *mec-4::gfp* transgene. (B) *madd-2; unc-6* and *unc-40; madd-2* double mutants exhibit no enhancement in AVM defects compared to single mutants (n = 73–297). (C) *madd-2;slt-1* double mutants exhibit enhanced defects compared to single mutants (n = 45–367). Error bars represent the standard error of proportion. Asterisks indicate different from single mutants by χ^2 test at $p < 0.01$. (D) Mutations in *madd-2* do not suppress the outgrowth phenotypes associated with MYR::UNC-40 expression. The percentage of excess AVM outgrowth, labeled by a *mec-4::gfp* transgene, was determined for animals carrying the MYR::UNC-40, MYR::UNC-40ΔP1, or MYR::UNC-40ΔP2 transgenes (Gitai et al., 2003) alone or as double mutants with *madd-2(ky592)* (n = 58–153). Error bars represent the standard error of proportion.

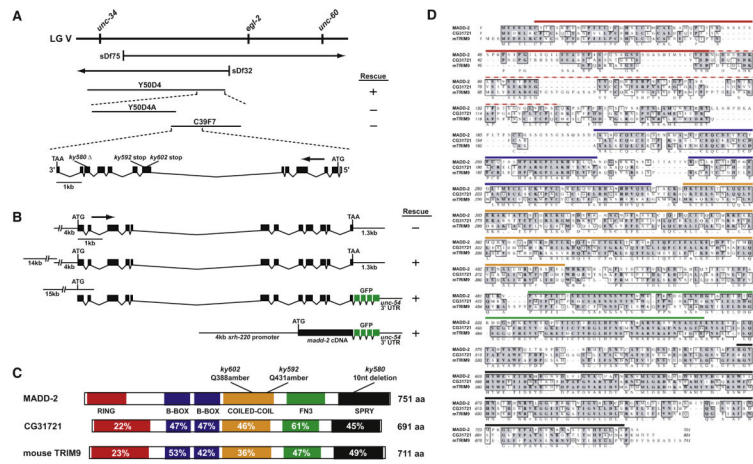


Figure 3. Molecular Analysis of *madd-2*

(A) Genetic map position of *madd-2*, deficiencies used for mapping, and clones used for rescue experiments, showing the genomic organization of the *madd-2* coding region with sites of mutations. Exons are indicated by black boxes and the 5' SL1 *trans*-splice leader sequence by an open box.

(B) *madd-2* genomic and cDNA subclones generated for rescue experiments and GFP expression studies.

(C) Predicted protein domains in MADD-2. The percent identities between MADD-2 and either CG31721 or mouse TRIM9 are shown for each domain. The sites of *madd-2* mutations are indicated.

(D) Amino acid sequence alignment for MADD-2, CG31721, and mouse TRIM9. The bars highlight the conserved domains and correspond to colors used for the domains shown in (C).

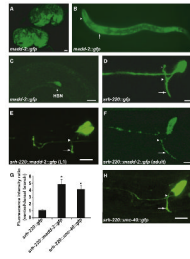


Figure 4. *madd-2::gfp* Expression and Preferential Localization of MADD-2 and UNC-40 to the ADL Ventral Branch

(A) Comma stage (bottom) and 1.5-fold stage (top) embryos. The anterior cells that express *madd-2::gfp* include developing neurons of the nerve ring. Expression is also detected in the ventral and posterior embryo, including motor neurons and hypodermal cells.

(B) L1 stage larva. Expression is high in head neurons that project into the nerve ring (arrow). Muscles of the head also express the transgene (arrowhead).

(C) L3 stage larva. The HSN motor neuron expresses the *madd-2::gfp* transgene.

(D) An *srh-220::gfp* transgene uniformly labels both dorsal (black arrowhead) and ventral (arrow) branches of the ADL neuron.

(E and F) In both larval (E) and adult (F) animals, the *srh-220::madd-2::gfp* transgene preferentially labels the ADL ventral branch (arrow).

(G) Quantitation of the fluorescence intensity ratio between the ventral and dorsal branches in adult animals expressing GFP, MADD-2::GFP, or UNC-40::GFP in ADL. Asterisks indicate a significant enrichment in ventral branch fluorescence as compared to GFP alone ($p < 0.005$, t test). Error bars represent the standard error of the mean.

(H) An L1 larva expressing *srh-220::unc-40::gfp* displays preferential expression of UNC-40::GFP in the ADL ventral branch (arrow).

For (D)–(F) and (H), the ADL branch point is indicated by a white arrowhead. Anterior is to the left and dorsal is at the top in all panels. Scale bars equal 5 μm .

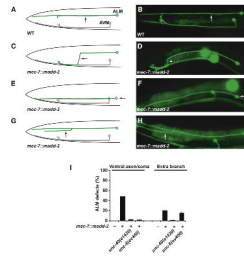


Figure 5. MADD-2 Overexpression Causes UNC-40-Dependent Ventral Outgrowth and Ectopic Branching of the ALM Neuron

(A and B) The ALM neuron projects an axon anteriorly to the head in a lateral position (arrow) in wild-type animals, as diagrammed or labeled by a *mec-4::gfp* transgene.

(C–H) *mec-7::madd-2(kyEx638)* transgenic animals: (C and D) the ALM axon projects to the ventral midline before reaching the nerve ring (arrow); (E and F) the ALM cell body (arrow) is ventrally displaced compared to wild-type; (G and H) the ALM axon exhibits an ectopic branch (arrow). Anterior is to the left and dorsal is at the top in all panels. Scale bar equals 5 μ m.

(I) ALM phenotypes in *madd-2*-overexpressing strains, with or without *unc-40* and *unc-6* mutations (n = 136–184). The same transgene, *mec-7::madd-2(kyEx638)*, rescues AVM and causes gain-of-function phenotypes in ALM. Error bars represent the standard error of proportion.

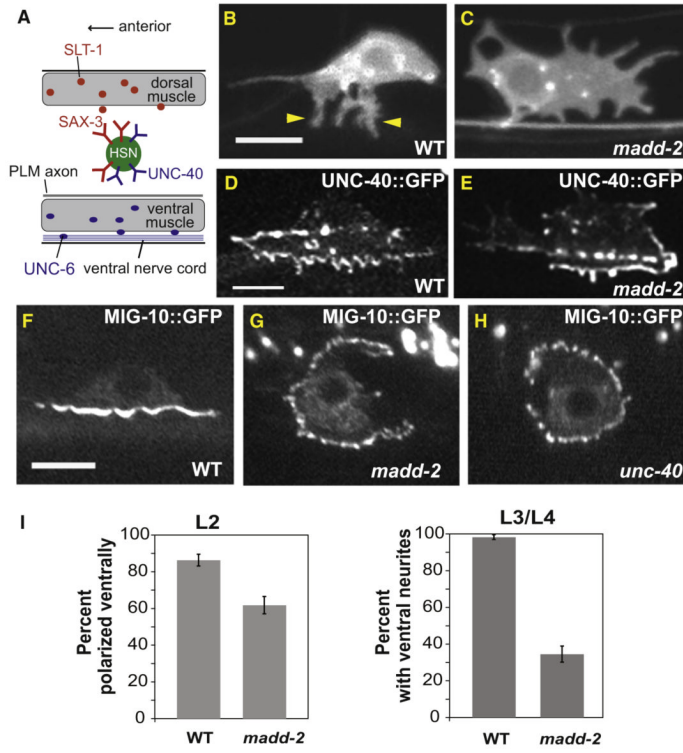



Figure 6. MADD-2 Is Required for Ventral MIG-10 Localization in HSN

(A) Diagram of molecules affecting HSN polarization and ventral guidance. (B and C) HSN neurons labeled with a membrane-bound GFP in L3 larval stage. (B) Wild-type animal with ventral HSN growth cones (arrowheads). (C) *madd-2* mutant with unpolarized HSN. (D and E) HSNs expressing functional, ventrally localized UNC-40::GFP protein in L3 larval stage wild-type (D) and *madd-2* mutant (E) animals. (F–H) HSNs expressing functional MIG-10::GFP protein in L3 larval stage wild-type (F), *madd-2* mutant (G), and *unc-40* mutant (H) animals. (I) Quantification of HSN defects at different developmental stages; polarized ventral growth in the L2 stage is followed by ventral neurite outgrowth in the L3 stage (Adler et al., 2006). Scale bars equal 5 μ m.

Table 1

Axon Branching and Guidance Defects in the ADL Amphid Neurons



	Wild-Type	No Ventral Branch	Ventral Route to Nerve Ring	n
Wild-Type	100%	0%	0%	217
<i>madd-2(ky580)</i>	43%	48%	9%	251
<i>madd-2(ky592)</i>	22%	62%	16%	361
<i>madd-2(ky602)</i>	21%	66%	12%	150
<i>unc-6(ky567)</i>	8%	83%	8%	53
<i>unc-6(ky577)</i>	39%	44%	8%	38
<i>unc-6(ky585)</i>	24%	67%	6%	51
<i>unc-6(ev400)</i>	11%	76%	13%	107
<i>unc-40(ky568)</i>	2%	71%	26%	46
<i>unc-40(ky591)</i>	2%	64%	29%	47
<i>unc-40(e271)</i>	8%	68%	24%	97
<i>unc-5(e53)</i>	100%	0%	0%	100
Wild-type (L1)	96%	4%	0%	55
<i>madd-2(ky592)</i> (L1)	11%	80%	9%	53
<i>unc-40(e271)</i> (L1)	0%	71%	29%	55
<i>madd-2(ky592); unc-6(ev400)</i>	9%	80%	13%	102
<i>unc-40(e271); madd-2(ky592)</i>	3%	78%	20%	75
<i>madd-2(ky592); srh-220::unc-40</i>	90%	10% ^a		227
<i>unc-40(e271); srh-220::madd-2</i>	0%	82%	17%	60

Amphid axon phenotypes were characterized using *srh-220::gfp* unless otherwise noted. Schematic drawings show the head, anterior to the left and dorsal at top. n is the number of neurons scored.

^a Scored with UNC-40::GFP marker, which did not distinguish between these two phenotypes.